

Vortex motion noise in micrometer-sized thin films of the amorphous $\text{Nb}_{0.7}\text{Ge}_{0.3}$ weak-pinning superconductor

D. Babić,^{1,*} T. Nussbaumer,¹ C. Strunk,^{1,†} C. Schönenberger,¹ and C. Sürgers²

¹*Institute of Physics, University of Basel, Klingelbergstrasse 82, CH-4056 Basel, Switzerland*

²*Physikalisches Institut, Universität Karlsruhe, D-76128 Karlsruhe, Germany*

(Received 22 November 2001; revised manuscript received 24 May 2002; published 24 July 2002)

We report high-resolution measurements of voltage (V) noise in the mixed state of micrometer-sized thin films of amorphous $\text{Nb}_{0.7}\text{Ge}_{0.3}$, which is a good representative of weak-pinning superconductors. There is a remarkable difference between the noise below and above the irreversibility field B_{irr} . Below B_{irr} , in the presence of measurable pinning, the noise at small applied currents resembles shot noise, and in the regime of flux flow at larger currents decreases with increasing voltage due to a progressive ordering of the vortex motion. At magnetic fields B between B_{irr} and the upper critical field B_{c2} flux flow is present already at vanishingly small currents. In this regime the noise scales with $(1 - B/B_{c2})^2 V^2$ and has a frequency (f) spectrum of $1/f$ type. We interpret this noise in terms of the properties of strongly driven depinned vortex systems at high vortex density.

DOI: 10.1103/PhysRevB.66.014537

PACS number(s): 74.76.Db, 74.40.+k, 74.60.Ge

I. INTRODUCTION

When set in motion by a current I , vortices in superconductors generate a voltage V . The resulting $V(I)$ curve may be either nonlinear, implying depinning phenomena, or linear, indicating flux flow (FF). Such $V(I)$ characteristics do not provide complete information on the nature of vortex motion, especially if the pinning is weak. This is a point where information available from the voltage noise becomes a powerful indicator of the underlying physics. The finding¹ that vortices moving as bundles composed of N magnetic-flux quanta ϕ_0 may produce shot noise attracted considerable attention, and resulted in extensive subsequent work which was eventually extended beyond a simple shot-noise approach.² Samples used in these studies were mainly polycrystalline conventional superconductors with appreciable pinning and nonlinear $V(I)$ characteristics up to very close to B_{c2} . Noise experiments have also been carried out on high- T_c superconductors,^{3–5} which are in a “liquid” state of negligible pinning over a large portion of the magnetic field vs temperature plane, displaying linear $V(I)$ curves. However, the intricate anisotropic character of vortex matter in these compounds is a serious obstacle to the understanding of the mechanisms that contribute to voltage noise related to motion of vortices against a weak pinning potential.

Thus a number of phenomena in the weak-pinning regime have remained largely unexplored from the point of view of vortex motion noise. The same holds for the noise properties in the depinned state, i.e., for $B > B_{irr}$. For instance, the interplay of bulk pinning and surface barriers,^{6,7} which are both obstacles for vortex motion (and can be of similar strengths when pinning is weak), has been studied mostly by analyzing the $V(I)$ curves and the magnetoresistance $R(B, T)$.⁸ Similarly, dynamic ordering of vortex motion has also been explored by measuring the average transport properties.⁹ Noise measurements can reveal effects which are beyond the reach of measurements of the average voltage. For example, if pinning is absent the $V(I)$ is linear, but one could ask does this mean that vortices really move completely “silently” or are there some dynamic effects which

introduce fluctuations in their velocity? Moreover, it is known that shot noise probes the properties of “granular magnetic-flux charge,” $N\phi_0$, but the details of this process are still subject to discussion—especially if N is small (characteristic of weak pinning).

In this paper we present high-resolution noise measurements which address the above topics. We have chosen a system particularly suitable for such research, namely $\text{Nb}_{0.7}\text{Ge}_{0.3}$ amorphous thin films of thickness d comparable to the coherence length ξ . These films are conventional, isotropic, weak-coupling s -wave BCS superconductors in the dirty limit, and for $\xi \sim d$ they exhibit an extended (B, T) range of easily movable vortices.¹⁰ In contrast to the complicated situation in high- T_c compounds, here vortices can be considered as undeformed “cylinders” of a volume $\xi^2 d$ and the Ginzburg-Landau (GL) parameters can be found straightforwardly. We also note that our shaping the samples in the form of *narrow wires* turned out to be crucial for observing the overall properties of the noise, i.e., for both $B < B_{irr}$ and $B > B_{irr}$.

In the regime where $V(I)$ and $R(B, T)$ still indicate the presence of pinning we find a noise similar to that in Ref. 11, i.e., which for small applied currents resembles shot noise, being linear in V and frequency independent at low frequencies, and decreases for more ordered vortex motion at high currents. Closer to B_{c2} , over a rather extended range, we find no evidence for pinning in neither $V(I)$ or $R(B, T)$. The lower boundary of this region is therefore taken as the irreversibility field B_{irr} . The noise for $B_{irr} < B < B_{c2}$ is qualitatively different from that in the presence of pinning. It exhibits a $1/f$ frequency spectrum and is quadratic in V . Moreover, it scales with $(1 - B/B_{c2})^2 V^2$. The monotonic increase with increasing V , and in particular the scaling which involves no pinning dependent parameters, motivates us to propose that the noise of this kind is a peculiar property of strongly driven vortices at high vortex density.

II. EXPERIMENT

Our samples (20 nm thick) were produced by magnetron sputtering of Nb and Ge on to oxidized silicon wafers

through masks prepared by electron-beam lithography, using a double layer resist (PMMA/PMMA-MA). The measurements were carried out in a ^4He cryostat, above the λ point of liquid helium. Voltage noise, $V(I)$ and $R(B, T)$, were measured extensively on a $W=5\text{-}\mu\text{m}$ -wide and $L=50\text{-}\mu\text{m}$ -long wire connected to two wide contact pads (sample S5). In order to investigate size effects in the noise we performed a less comprehensive set of measurements on a $W=1\text{ }\mu\text{m}$ and $L=10\text{ }\mu\text{m}$ sample (sample S1). By analyzing the low-current (10 nA ; 10 A cm^{-2}) $R(B, T)$ measurements within the framework of a model appropriate for dirty weak-coupling superconductors¹² we characterized sample S5 in detail. The transition temperature $T_c=2.91\text{ K}$ is determined as the midpoint of the 10%–90% (0.1 K) zero-field transition curve. The transition curve is smooth and free of “kinks” that would indicate the presence of inhomogeneities, and we ascribe the rather wide transition (in units of T/T_c) to a pronounced two-dimensional character of the sample. A similar conclusion was drawn in Ref. 13 for a $\text{YBa}_2\text{Cu}_3\text{O}_{7-\delta}$ single crystal investigated systematically with respect to different δ -values and consequently different anisotropies. Very weak temperature dependence of the normal-state resistivity ρ_N above T_c permits the estimation of $\rho_N(T=0)=(2.3 \pm 0.2)\text{ }\mu\Omega\text{ m}$. Using this value and $-(dB_{c2}/dT)_{T=T_c} \approx 2.05\text{ TK}^{-1}$, determined from the $R(B=\text{const.}, T)$ measurements (not shown), we calculate¹² the GL parameters: $\xi(0)=7.4\text{ nm}$, $\kappa=77$, and $\lambda(0)=1.63\kappa\xi(0)=930\text{ nm}$. The parameters of sample S5 are in good agreement with published work.¹⁰ Sample S1 had a slightly lower T_c (2.55 K) and larger ρ_N , but otherwise showed fairly the same properties as sample S5. The method of noise measurements is described in detail in Ref. 14. In short, the signal from a sample is processed through two low-noise amplifiers the outputs of which are cross correlated in a spectrum analyzer. The noise setup is calibrated against the equilibrium Nyquist noise $4k_B TR_N$ in the normal state (R_N is the normal state resistance). By this approach we have obtained a resolution of $\approx 10^{-20}\text{ V}^2\text{ s}$, necessary for measurements of small noise signals appearing in the case of weak pinning. For both samples the frequency window for the noise measurements was 106.5–114 kHz, except for the measurements of the frequency dependence of the noise power spectrum S_V , performed at several frequencies between 20 and 250 kHz.

All the noise measurements were carried out at fixed temperatures, $T=2.4\text{ K}$ ($T/T_c=0.82$) for sample S5 and $T=2.25\text{ K}$ ($T/T_c=0.88$) for sample S1. Since sample S1 had lower T_c , we had to choose a larger value of T/T_c in order to avoid temperature instabilities that appear in the vicinity of the λ point.

III. MAGNETORESISTANCE AND CURRENT-VOLTAGE CHARACTERISTICS

First we analyze the $R(B, T)$ and $V(I)$ results. In the lower inset to Fig. 1 we show $R(B, 2.4\text{ K})$ for sample S5. Above $\sim 0.65\text{ T}$ we found good agreement with the FF theory of Larkin and Ovchinnikov (LO).¹⁵ The LO FF conductivity is given by

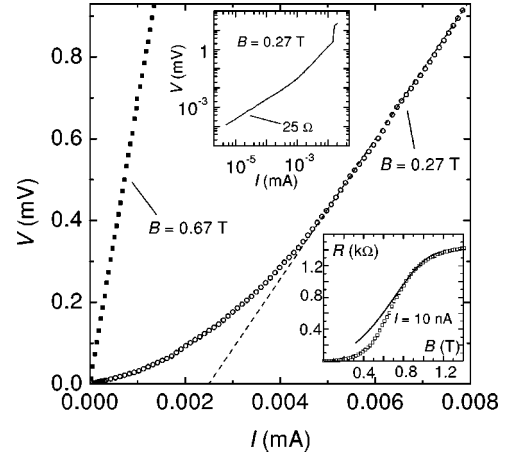


FIG. 1. $V(I)$ at 0.27 T (open circles) and 0.67 T (full squares) for sample S5 at 2.4 K. At 0.27 T, for large currents there is a $V \propto (I - I_c)$ dependence (indicated by the dashed line). At 0.67 T and higher fields the $V(I)$ are linear starting from $I \rightarrow 0$ and over the whole range of our noise measurements. Upper inset: Log-log plot of our noise measurements, showing, at small currents, Ohmic behavior (with $R=25\text{ }\Omega$) over two decades in I , and a jump to a value close to $V_N=R_N I$ at high currents. Lower inset: $R(B, 2.4\text{ K})$. The solid line is the LO FF resistance drawn using $T_c=2.91\text{ K}$, $B_{c2}=1.18\text{ T}$, and $R_N=1375\text{ }\Omega$.

$$\sigma_{FF} = \frac{1}{\rho_N} \left[1 + \frac{1}{(1 - T/T_c)^{1/2}} \left(\frac{B_{c2}}{B} \right) g(B/B_{c2}) \right], \quad (1)$$

where (for $z > 0.315$) $g(z) = (1 - z)^{3/2} [0.43 + 0.69(1 - z)]$. The solid line, representing the LO FF resistance $R_{FF} = R_N / \sigma_{FF} \rho_N$, is drawn by taking $T_c=2.91\text{ K}$, $B_{c2}=1.18\text{ T}$, and $R[B_{c2}(2.4\text{ K})] = R_N = 1375\text{ }\Omega$ ($\rho_N = 2.75\text{ }\mu\Omega\text{ m}$). The mentioned uncertainty in ρ_N implies a certain range of the B_{c2} values that do not deteriorate the fit. This range is $\sim 1.14\text{--}1.22\text{ T}$ and agrees fairly well with $B_{c2} \sim 1.09\text{--}1.12\text{ T}$ obtained by the extrapolation method of Ref. 9. Henceforth we use $B_{c2}=1.18\text{ T}$. Taking different values of T_c (within the transition width) has little effect on the quality of the fit. We conclude that for the fields above $\sim 0.65\text{ T}$ the vortices flow freely even at very small applied currents, and thus $B_{irr}(2.4\text{ K}) \sim 0.65\text{ T}$, which is, as we show below, in agreement with the $V(I)$ results.

For magnetic fields below $\sim 0.65\text{ T}$ the LO theory does not explain the magnetoresistance data, and R is smaller than R_{FF} . This indicates that the vortices are slowed down by experiencing a pinning potential. However, R is finite even at magnetic fields as low as $\sim 0.05 B_{c2}$, which implies a very weak pinning. In the upper inset to Fig. 1 we show a log-log plot of a typical $V(I)$ in this region, for 0.27 T. Over two decades in I the $V(I)$ is Ohmic ($R=25\text{ }\Omega$) before it turns upwards. This suggests a hopping vortex motion (HVM), most probably thermally activated. In the model of thermally activated HVM, vortex velocity is given by $v_\phi = l(\nu_+ - \nu_-)$, where l is the hop length and $\nu_\pm \propto \exp[-(U \mp U_F)/k_B T]$ the hopping rates over a potential U in the direction (+) and opposite (-) to the driving force $\mathbf{F} = -\nabla U_F$. Since $F \propto IB$ and $V = BLv_\phi$, for $I \rightarrow 0$ the $V(I)$ is linear.

From our measurements of $R(B=\text{const.}, T)$ we can estimate the values of U/k_B , which are remarkably small. At 2.4 K, U/k_B is lower than 10 K and is a decreasing function of B . At higher currents the $V(I)$ gradually changes to a $V(I) \propto (I - I_c)$ dependence, as we show for 0.27 T in Fig. 1 by open circles. This suggests a force-induced transition to flux flow, i.e., an ordering of the vortex motion with increasing driving force. This assumption will be supported further by the noise results presented in Sec. IV A. Finally, at even higher currents V jumps to a value of the order of $V_N = R_N I$ (Fig. 1, upper inset) due to the appearance of nonlinear FF described in the LO theory¹⁵ and observed experimentally for similar films.^{9,16} Above 0.65 T, where FF takes place even at vanishingly small currents, the $V(I)$ is simple: linear starting from $I \rightarrow 0$ and all the way up to the appearance of nonlinear effects in FF, as shown for 0.67 T in Fig. 1 by full squares.

IV. NOISE RESULTS

In the rest of the paper we present and discuss the results of our noise measurements, which if not specified otherwise refer to sample S5. We introduce Σ_V to denote the excess noise, which is the difference between the total measured noise S_V and the thermal (Nyquist) noise $4k_B T(dV/dI)$. The currents used in the noise measurements were always kept below those corresponding to the appearance of the high-current nonlinearities mentioned in Sec. III, since we are interested in situations where the average transport properties are still unaffected by the high-current dynamical processes described in the LO theory.¹⁵ In Sec. IV A we analyze the noise in the regime of nonlinear $V(I)$ curves, i.e., for $B < B_{irr}$, and in Sec. IV B we turn to the noise for $B_{irr} < B < B_{c2}$, where the $V(I)$ is linear and $R(B, 2.4 \text{ K})$ agrees well with the LO FF theory.

A. Noise in the regime of nonlinear $V(I)$

In Fig. 2 we show a typical $\Sigma_V(V)$ curve in the regime of nonlinear $V(I)$, i.e., for 0.27 T [corresponding to the $V(I)$ curve in Fig. 1]. The maximum background Nyquist noise is $\sim 2.5 \times 10^{-20} \text{ V}^2 \text{ s}$. $\Sigma_V(V)$ first increases linearly up to $V \approx 0.2 \text{ mV}$ which is close to the upper limit of HVM in $V(I)$. At higher voltages, where $V(I)$ becomes proportional to $(I - I_c)$, Σ_V gradually decreases with increasing V . From this decrease of $\Sigma_V(V)$ we infer that the vortex motion becomes more and more ordered when the driving force progressively dominates over the pinning potential. At large driving force the pinning potential causes not only a finite offset I_c in $V(I)$ but also random fluctuations of the vortex velocity, which is most probably the origin of the small residual noise above $V \sim 0.5 \text{ mV}$. This residual noise is expected to vanish together with I_c at B_{irr} , which is indeed observed in our experiment. It is worthwhile to note that the onset of collective vortex motion has stronger effect on Σ_V than on $V(I)$. In Σ_V the depinning threshold I_c is indicated by a pronounced maximum above which an ordering of the vortex motion occurs. On the other hand, $V(I)$ shows no sharp feature at I_c , implying that I_c has to be determined by extrapolation of

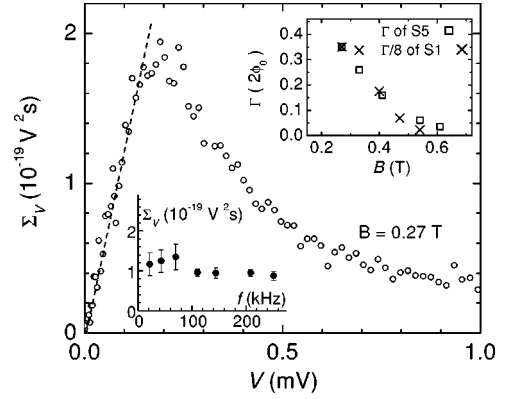


FIG. 2. Vortex motion noise $\Sigma_V(V)$ at 0.27 T and $T=2.4 \text{ K}$, corresponding to the $V(I)$ curve in Fig. 1. The dashed line indicates the linear $\Sigma_V(V)$ dependence. Lower inset: $\Sigma_V(f)$ measured at 0.33 T and $1 \mu\text{A}$ ($65 \mu\text{V}$), in the linear part of $\Sigma_V(V)$. Upper inset: Magnetic-field dependences of the slopes Γ (expressed in units of $2\phi_0$) of the linear $\Sigma_V(V)$ curves. The values for sample S1 divided by eight (crosses) agree well with those for sample S5 (squares), which is in fair agreement with the assumption that Γ is inversely proportional to sample width.

the linear part of $V(I)$ down to $V=0$. Since the linear regime extends only over a small current range between the HVM regime and the high-current nonlinearities, the determination of I_c is more ambiguous than in Σ_V . The nonmonotonic character of $\Sigma_V(V)$ supports our interpretation more strongly, and also supplements research on dynamic vortex ordering studied⁹ by analyzing the average transport properties.

Similarly to shot noise (in current) of electrons, which is a linear function of I , shot noise (in voltage) of vortices is a linear function of V .¹ To check whether the linear increase of $\Sigma_V(V)$ in the low-voltage regime can be interpreted as shot noise we investigated the frequency and sample-width dependences of Σ_V . The studies^{1,11,17} of vortex motion shot noise offer different models for the slopes Γ of linear $\Sigma_V(V)$ plots, as we discuss later, but they agree in predicting a frequency-independent $\Sigma_V(f)$ up to a frequency $f_c \sim v_\phi/W = V/BLW$. Because the wire width W is small, in the present case the (calculated) f_c is large, more than 500 kHz for all the measured points, except for a few ones very close to $V=0$. We measured $\Sigma_V(f)$ at a characteristic point ($V = 65 \mu\text{V}$) of a linear $\Sigma_V(V)$ curve, and found that $\Sigma_V(f)$ is essentially flat between 20 and 250 kHz, as shown in the lower inset to Fig. 2. This result meets the above-mentioned expectation for shot noise.

In an earlier work¹ on vortex shot noise the factor Γ was related to the “charge” of a vortex bundle, i.e., $\Gamma = 2N\phi_0$. The low level of noise found in this study for Corbino disc geometry implied that the noise in the samples of bar geometry was produced essentially at their edges. This finding can be understood in terms of the surface barriers (of Bean-Livingston⁶ or geometrical⁷ type) for a vortex entering and leaving a sample. In short, a depinned vortex bundle “shoots” across a bar-geometry sample, interacts only weakly with the pinning centers and the rest of (pinned or slowly moving) vortices, and the noise is created by the

bundle overcoming the barriers at the entry and exit from the sample. In this case Γ does not depend on sample width. However, in later studies^{11,17} it was found that if vortex bundles travel a distance $x \ll W$ before their motion is interrupted by the pinning centers, Γ should be inversely proportional to W . The reason for this can be inferred from the Josephson relation $V = \phi_0(d\varphi/dt)/2\pi$, where φ is the phase of the superconducting order parameter. A moving vortex causes the phase shift of 2π only if it moves over the whole distance W . If the actual distance x is shorter than W , the phase change associated with one voltage pulse is a factor x/W less than 2π , and the consequence is $\Gamma = 2\phi_0 N x/W$.¹⁷ Note that in this case the noise is produced in the bulk, i.e., at the pinning centers. The reduction factor x/W explains the result of Ref. 1 that the noise produced in the bulk (by slow vortices moving over small distances, or by local bundle-velocity fluctuations) was much smaller than that due to the “shooting” bundles overcoming the surface barriers. A more complicated expression for Γ was derived in Ref. 11, where it was found that if there is a distribution of the strengths and positions of pinning centers the above expression becomes $\Gamma = 2\phi_0 \langle N^2 \rangle \langle x^2 \rangle / \langle N \rangle \langle x \rangle W$, where the brackets denote averages over the distribution function.

In the upper inset of Fig. 2 we plot $\Gamma(B)$ for sample S5 and $\Gamma(B)/8$ for sample S1. Over the whole field range where we found well defined linear $\Sigma_V(V)$ curves the slopes $\Gamma(B)$ for both samples decrease with increasing field in the same manner, and Γ for sample S1 is approximately eight times larger. If we take into account slightly different experimental conditions for the two samples this is in fair agreement with $\Gamma \propto 1/W$. At magnetic fields lower than ~ 0.20 T the resistances of the samples, the measured voltage and the corresponding voltage noise are small, which leads to a large error in Γ .

We now address the question of whether the noise is produced by the pinning or by the surface barriers. The surface barriers are important at applied magnetic fields of the order of, or lower than, the thermodynamic critical field $H_c = B_{c2}/\mu_0\kappa\sqrt{2}$. In our case, $\mu_0 H_c \sim 11$ mT is much lower than the fields at which we found the noise of a measurable magnitude. In addition, the approximate scaling of Γ with sample width suggests that the bulk pinning, and not the sample edges, dominates the noise. In turn, measurements of the width dependence of Γ may be an alternative to other experiments⁸ for determining whether the surface barriers influence the measured transport properties.

The fact that our measurements allow us to exclude the surface barriers as the main origin of the noise in our samples also sheds more light on the nature of the B_{irr} and the meaning of the potential U of HVM. It is known that for some samples (e.g., single crystals of the $\text{Bi}_2\text{Sr}_2\text{CaCu}_2\text{O}_{8+x}$ high- T_c superconductor) surface barriers may have considerable effect on both the irreversibility field¹⁸ and the thermally activated transport.⁸ This is not the case in the present situation, the B_{irr} can be attributed to a transition to a depinned vortex state and the U is related to bulk pinning, as we have anticipated in Sec. III.

We attribute the decrease of Γ with increasing B to the weakening of pinning as B approaches B_{irr} , since for $B > B_{irr}$ we found no linear $\Sigma_V(V)$ curves and, moreover, the overall noise magnitude decreases as B increases towards B_{irr} . The decrease of $\Gamma(B)$ for B well below B_{irr} could be explained within the framework of the models of Refs. 11 and 17, if the unknown parameters $\langle x \rangle, \langle x^2 \rangle, \langle N \rangle, \langle N^2 \rangle$, and, respectively, x, N depend on magnetic field in the right way. Since Γ comprises these parameters as products and ratios (see above), they cannot be extracted independently from our data. However, both models break down in the limit $B \rightarrow B_{irr}$. This can be understood as follows. The effects of pinning are (i) formation of vortex bundles in order to increase the driving force and thus facilitate their motion against the pinning potential, (ii) reduction of the hopping distance below the sample width W . The pinning force vanishes at B_{irr} , implying $\langle N^2 \rangle^{1/2} \rightarrow \langle N \rangle \rightarrow 1$ and $\langle x^2 \rangle^{1/2} \rightarrow \langle x \rangle \rightarrow W$, i.e., $\Gamma \rightarrow 2\phi_0$, which is in contrast to the experimental observation shown in Fig. 2.

A reason for this breakdown of the classical models can possibly be inferred from the comparison of the transports of (normal) electrons and vortices close to the limit of perfect transmission. Our experimental realization, where vortices are created at the entry into a sample and vanish at the exit, is equivalent to a two-terminal mesoscopic conductor—where electrons have their source and drain in the reservoirs. Whenever the transmission coefficient Θ for electron transport through such a mesoscopic conductor is close to unity, shot noise is suppressed by a factor $(1 - \Theta)$.¹⁹ In the ballistic limit ($\Theta = 1$) there is no noise associated with electron transport. If vortices are not slowed down by bulk pinning and/or surface barriers, their motion is determined by the viscous drag only. This situation represents perfect vortex motion, conceptually similar to ballistic transport of electrons. Therefore, if there are no dynamic effects present (see Sec. IV B), in the limit of perfect vortex transmission across a sample the noise should vanish. A more quantitative treatment of vortex motion shot noise at high transmittance requires further research.

B. Noise in the regime of linear $V(I)$

Above $B_{irr} \sim 0.65$ T, where the vortex density is large and $V \approx R_{FF}I$ for all our noise measurements, no noise described in Sec. IV A was found. Instead, as we show in Fig. 3(a), Σ_V is a monotonic function of V , increasing as V^2 , and as a function of magnetic field it decreases as B approaches B_{c2} . Moreover, as shown in Fig. 3(b), there is a scaling $\Sigma_V \propto (1 - B/B_{c2})^2 V^2$ which holds over $B_{irr} < B < B_{c2}$ and is insensitive to variations of B_{c2} in the range 1.14–1.22 T. The frequency dependence of Σ_V in this regime is of $1/f$ type, more precisely $1/f^\alpha$ with $\alpha = 1.5 \pm 0.1$ [Fig. 3(b), upper inset]. In the normal state, above B_{c2} , $\Sigma_V = 0$ and S_V is simply the voltage-independent Nyquist noise.

The existence of any noise in the regime where the vortices are most likely to be completely depinned, as seen from the $R(B, T)$ and $V(I)$, is rather surprising, since in the pinned state the magnitude of the noise described in Sec. IV A is becoming progressively smaller as $B \rightarrow B_{irr}$. Furthermore, if

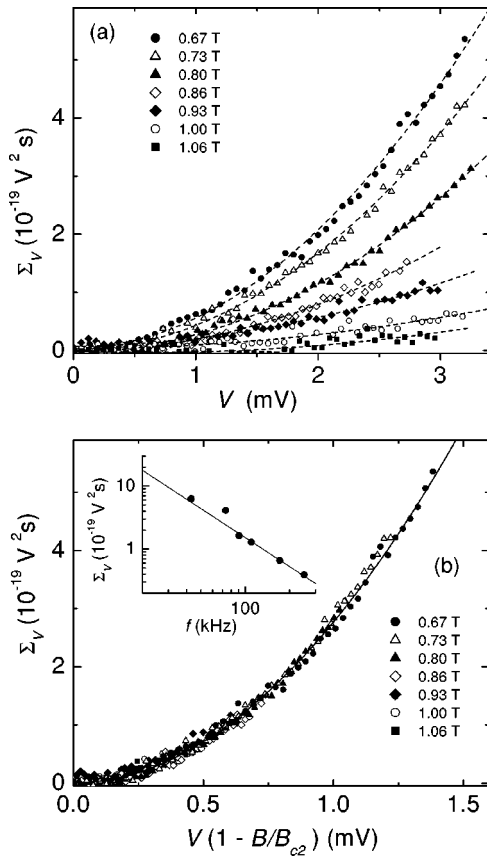


FIG. 3. (a) Vortex motion noise $\Sigma_V(V)$ for $0.67 \text{ T} \leq B \leq 1.06 \text{ T}$. The dashed lines are fits to $\Sigma_V \propto V^2$ dependence. (b) The curves from (a) plotted against $(1 - B/B_{c2})V$. Solid line: $\Sigma_V = \gamma(1 - B/B_{c2})^2 V^2$ with $\gamma(110 \text{ kHz}) = 2.1 \times 10^{-13} \text{ s}$. Upper inset: Frequency dependence of this noise, measured at 0.67 T and 1.5 mV , showing $\Sigma_V(f) \propto f^{-\alpha}$ with $\alpha = 1.5 \pm 0.1$, as indicated by the solid line.

the background pinning would still influence the noise significantly one would not expect an increase of Σ_V with increasing V , because at larger driving force the role of pinning is less important. Therefore the origin of the noise shown in Fig. 3. has to be sought in dynamic properties of depinned vortices far from equilibrium, with a guideline along the LO theory of nonequilibrium phenomena in flux-flow dissipation.¹⁵ In addition, a possible partial or complete melting of the vortex lattice, which could occur at B_{irr} ,¹³ should also be taken into account.

There is experimental evidence in support of our assumption that the peculiar noise observed is not related to depinning processes. In Fig. 4 we show $\Sigma_V(V)$ for 0.61 T , i.e., just at the crossover from HVM to LO FF in $R(B, T)$. For low voltages, $\Sigma_V(V) \propto V$ (as indicated by the dashed line), suggesting that the vortices undergo the HVM. At $V \sim 0.8 \text{ mV}$ the noise starts to deviate from the linear dependence, showing in a small voltage range a tendency to decrease, typically for the vortex motion becoming more ordered with increasing driving force. However, at higher V the decrease of $\Sigma_V(V)$ does not continue but instead Σ_V approaches the same $\Sigma_V(V) \propto V^2$ behavior as for the higher fields [the solid line in Fig. 4 indicates the scaling in Fig. 3(b)]. Although the

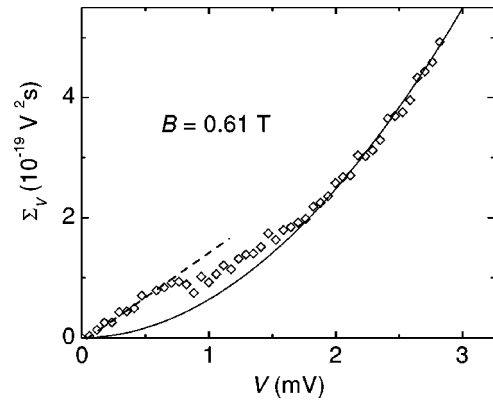


FIG. 4. Vortex motion noise $\Sigma_V(V)$ for 0.61 T , i.e., for B slightly below B_{irr} . For small V , $\Sigma_V \propto V$, as indicated by the dashed line. Above $V \sim 0.8 \text{ mV}$ the noise in a rather narrow voltage range decreases with increasing V , but then increases again at higher voltages. Eventually, the increase becomes quadratic in V and approaches the same scaling as for $B > B_{irr}$, shown by the solid line.

vortex motion is becoming more and more uniform the noise increases, which can hardly be explained in terms of vortex interaction with a pinning potential.

Quadratic voltage dependence and $1/f$ power spectrum are generally known to be the properties of resistance fluctuations.²⁰ Hence a possibility that our finding represents resistance fluctuations, i.e., vortex velocity fluctuations, requires attention. At a fixed (B, T, I) point, two parameters influence vortex velocity and consequently FF resistance: ρ_N and vortex core area A_c . Thus if there are fluctuations in either ρ_N or A_c , the FF resistance fluctuates as well. The fact that the measured noise above B_{c2} is just the Nyquist noise rules out fluctuations of ρ_N , leaving us with a possibility that A_c fluctuates. We argue below that such fluctuations may occur if the vortex velocity is large and the vortex density high.

The nonequilibrium properties of vortex cores and the related influence on flux-flow dissipation were studied theoretically by LO,¹⁵ and in Ref. 21. If the electric field generated in moving vortex cores is sufficiently strong, quasiparticles in the cores can gain enough energy to overcome the potential barriers at vortex edges and to escape into the surrounding superfluid. This leads to a reduction of the core size, the vortex viscosity decreases,²² and the vortex velocity increases, resulting in the nonlinearities in $V(I)$ at large currents and finally the jump shown in the upper inset to Fig. 1. At low vortex density the electron-phonon relaxation processes are sufficiently efficient to cool the hot quasiparticles to the bath temperature, as the heating occurs in the cores only and the cooling over the whole volume.

However, the situation changes at *large vortex density*. With increasing vortex density the cooling efficiency decreases and the quasiparticles are heated-up to an elevated temperature.^{15,21} This may cause an increase of thermal fluctuations of the quasiparticle density. As a consequence, the quasiparticle pressure on the vortex “walls” may fluctuate, which would then result in the fluctuations of A_c . The related fluctuations of v_ϕ are measured as voltage fluctuations.

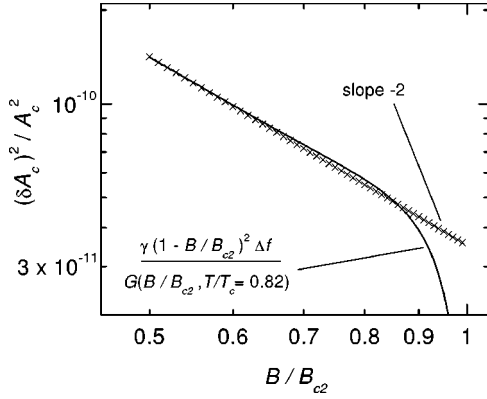


FIG. 5. Solid line: log-log plot of $(\delta A_c)^2/A_c^2$ given by Eq. (3), for $f=110$ kHz, $\Delta f=7.5$ kHz, $T/T_c=0.82$, $\gamma=2.1 \times 10^{-13}$ s [corresponding to the data shown in Fig. 3(b)]. Crosses indicate the $(B/B_{c2})^{-2}$ approximation of $(\delta A_c)^2/A_c^2$, discussed in the text.

Since the average transport properties can be for $B > B_{irr}$ consistently described by the LO theory, it is tempting to check whether the LO expression for σ_{FF} (see Sec. III) allows us to relate the possible core-size fluctuations and the measured fluctuations in voltage. Because the observed noise occurs where $V(I)$ is linear, the $\Sigma_V \propto V^2$ dependence can be explained by assuming fluctuations of the conductivity, i.e., $\Sigma_V \Delta f = (\delta V)^2 = (\delta \sigma_{FF})^2 / \sigma_{FF}^2 V^2$. Δf is the frequency interval over which the noise spectrum is averaged. To relate the fluctuations $\delta \sigma_{FF}$ and δA_c we can rewrite σ_{FF} in terms of the vortex core area $A_c \sim \xi^2 \sim \phi_0 / B_{c2}$ and the intervortex distance $l_B \sim \sqrt{\phi_0 / B}$, so that $z = B/B_{c2} = A_c / l_B^2$. Then we calculate $\delta \sigma_{FF} = (1/l_B^2)(\partial \sigma_{FF} / \partial z) \delta A_c$ from Eq. (1) and obtain

$$\frac{(\delta \sigma_{FF})^2}{\sigma_{FF}^2} = G(B/B_{c2}, T/T_c) \frac{(\delta A_c)^2}{A_c^2}, \quad (2)$$

where $G(z, T/T_c) = [dg(z)/dz - g(z)/z]^2 / [(1 - T/T_c)^{1/2} + g(z)/z]^2$.

The form of $(\delta A_c)^2/A_c^2$ is not known *a priori*. However, it can be deduced by combining Eq. (2) and the experimentally observed behavior $(\delta \sigma_{FF})^2 / \sigma_{FF}^2 = (\delta V)^2 / V^2 = \gamma(1 - B/B_{c2})^2 \Delta f$ [see Fig. 3(b)]. This results in

$$\frac{(\delta A_c)^2}{A_c^2} = \gamma \frac{(1 - B/B_{c2})^2 \Delta f}{G(B/B_{c2}, T/T_c)}. \quad (3)$$

In Fig. 5 we plot this expression against B/B_{c2} in order to check whether there is any approximation that would lead to a simple picture of the fluctuations. It is seen that $(\delta A_c)^2/A_c^2$ can be well approximated for $B/B_{c2} \leq 0.92$ by a power law, i.e., $(\delta A_c)^2/A_c^2 \propto (B/B_{c2})^{-n}$ with $n \approx 2$. The simulations for other values of T/T_c show that the power-law approximation holds well for essentially any value of T/T_c . The power n weakly depends on T/T_c but is reasonably close to 2 in the region $0.7 < T/T_c < 0.95$.

The apparent $(B/B_{c2})^{-2}$ decrease of $(\delta A_c)^2/A_c^2$ has a simple visualization: such a functional dependence corresponds to a plausible assumption that the fluctuations δA_c of

the vortex area are proportional to the space $\sim l_B^2$ available, so that $(\delta A_c)/A_c \propto (l_B^2/\xi^2) \propto (B/B_{c2})^{-1}$. The above modeling based on the LO conductivity hence shows that the assumption of core-size fluctuations may reproduce the measured voltage and magnetic-field dependences of the voltage noise.

With the experimentally determined value of the prefactor $\gamma = 2.1 \times 10^{-13}$ s for $f = 110$ kHz and $\Delta f = 7.5$ kHz we obtain the relative fluctuation amplitude $\delta A_c/A_c$ of the order of 10^{-5} . However, as we discuss below, the $1/f$ spectrum implies that the fluctuations are distributed over a range of relaxation times. As a consequence, the small value of $\delta A_c/A_c$ only represents the contribution of those core-size fluctuations which occur in this frequency window around the given frequency.

The observed $1/f$ spectrum cannot be explained if all vortex cores fluctuate in exactly the same manner. The fluctuation of the size of a vortex core is assumed to be a random process with a characteristic time τ . If τ would be the same for all cores, this would result in a Debye-Lorentzian spectrum of the fluctuations, white up to the cutoff frequency $1/\tau$. On the other hand, a distribution of τ and a superposition of Debye-Lorentzian spectra may result in a $1/f$ spectrum.²⁰ Properties of the distribution then also determine how much the fluctuations with a given τ contribute to $\delta A_c/A_c$ measured at $(f, \Delta f)$. Such a distribution may arise, for example, as a consequence of *different local correlations*.

That vortex motion can strongly depend on local conditions was demonstrated in Ref. 23, where it was found that, in the presence of pinning, vortices move in a form of intermittent “rivers” between the pinned islands. In our case one can hardly discuss a motion around the pinned islands, since any important pinned fraction would affect the average transport properties significantly, which is not observed (see the discussion of Fig. 1). This, however, does not necessarily imply that there are no “floating islands,” i.e., vortex lattice domains moving together with the “liquid” phase. The average flux-flow dissipation in such a (depinning) system would be still well described by the LO theory, since the ratio B/B_{c2} influences the magnetoresistance much more strongly than the exact geometry of a system of moving vortices.¹⁵ However, *the local vortex correlations could be different* for vortices deeply in the islands, in the liquid, close to the island boundaries, etc., which could lead to different relaxation times for the core fluctuations. These different relaxation times would then give a $1/f$ noise spectrum.

We are aware that our arguments offer only a qualitative picture, and that further clarification of the above ideas is required. However, at the moment we do not know of any quantitative theoretical model which would account for the observed peculiarities of vortex motion noise above B_{irr} , nor are we aware of any related systematic experimental work dealing with a range $B_{irr} < B < B_{c2}$ as large as $\sim 50\%$ of B_{c2} . Thus we believe that the results and discussion of this section could be used as a possible starting point for further experimental and theoretical work.

V. SUMMARY AND CONCLUSIONS

We have measured voltage noise in the mixed state of micrometer-sized wires of amorphous $\text{Nb}_{0.7}\text{Ge}_{0.3}$ thin films.

The samples are well described by conventional theories for dirty weak-coupling superconductors, have weak pinning, relatively low irreversibility field B_{irr} , and the vortex structure is much simpler than in high- T_c superconductors. These properties make the samples suitable for exploring the vortex motion noise in the weak-pinning regime.

At low magnetic fields, i.e., for $B < B_{irr}$, and small applied currents the voltage-current curves exhibit properties characteristic of thermally activated hopping of vortices. The related noise is a linear function of voltage, with the slopes Γ of noise vs voltage curves inversely proportional to the sample width, and is basically frequency independent up to 250 kHz. This behavior is in agreement with the shot noise model and the assumption that the noise is generated by bulk pinning and not by surface barriers. Γ decreases with increasing B over the whole magnetic field range of the shot-noise-like behavior, which does not contradict the presently available models of vortex motion shot noise. These models, however, fail to explain the disappearance of the shot noise as $B \rightarrow B_{irr}$. For $B < B_{irr}$ but at larger currents the vortex motion becomes more uniform and the noise decreases. The decrease and the low level of the noise is ascribed to the ordering of vortex motion with increasing driving force.

In a narrow range of B slightly below B_{irr} , at low V one

still observes the above-mentioned two types of noise but at large V the noise becomes quadratic in V . This signifies the appearance of the dynamic effects inherent to large vortex density, a behavior fully developed for $B > B_{irr}$. For $B > B_{irr}$ the $V(I)$ curves are linear over the whole range of our measurements and the magnetoresistance agrees well with the flux-flow theory of Larkin and Ovchinnikov. The noise in this regime is completely different from that for $B < B_{irr}$. Over the whole voltage range it increases quadratically with increasing voltage, its frequency spectrum is of $1/f$ type, and it scales with $(1 - B/B_{c2})^2 V^2$. The origin of this noise is not entirely clear. We present a qualitative explanation in terms of the nonequilibrium properties of moving vortex cores which are subjected to fluctuations of their radius.

ACKNOWLEDGMENTS

We are grateful to J. Aarts for contributing to this work in its initial stage. Valuable discussions with K. E. Nagaev, V. B. Geshkenbein, G. B. Lesovik, G. Blatter, H. v. Löhneysen, F. Nori, E. H. Brandt, and J. R. Cooper are gratefully acknowledged. This work was supported by the Swiss National Science Foundation.

*Corresponding author. Present address: Department of Physics, Faculty of Science, University of Zagreb, Croatia. Electronic address: dbabic@phy.hr

[†]Present address: Institute for Experimental and Applied Physics, University of Regensburg, Germany.

¹D. J. van Ooijen and G. J. van Gurp, Phys. Lett. **17B**, 239 (1965); G. J. van Gurp, Phys. Rev. **166**, 436 (1968).

²For an overview, see J. R. Clem, Phys. Rep. **75**, 1 (1981). This paper also contains details of a theoretical approach to vortex motion noise.

³P. J. M. Wöltgens, C. Dekker, S. W. A. Gielkens, and H. W. de Wijn, Physica C **247**, 67 (1995).

⁴G. D'Anna, P. L. Gammel, H. Safar, G. B. Alers, D. J. Bishop, J. Giapintzakis, and D. M. Ginsberg, Phys. Rev. Lett. **75**, 3521 (1995).

⁵D. H. Kim, K. E. Gray, N. Jukam, D. J. Miller, Y. H. Kim, J. M. Lee, J. H. Park, and T. S. Hahn, Phys. Rev. B **60**, 3551 (1999).

⁶C. P. Bean and J. D. Livingston, Phys. Rev. Lett. **12**, 14 (1964).

⁷E. Zeldov, A. I. Larkin, V. B. Geshkenbein, M. Konczykowski, D. Majer, B. Khaykovich, V. M. Vinokur, and H. Shtrikman, Phys. Rev. Lett. **73**, 1428 (1994).

⁸D. T. Fuchs, R. A. Doyle, E. Zeldov, S. F. W. R. Rycroft, T. Tamegai, S. Ooi, M. L. Rappaport, and Y. Myasoedov, Phys. Rev. Lett. **81**, 3944 (1998); S. F. W. R. Rycroft, R. A. Doyle, D. T. Fuchs, E. Zeldov, R. J. Drost, P. H. Kes, T. Tamegai, S. Ooi, and D. T. Foord, Phys. Rev. B **60**, R757 (1999).

⁹J. M. E. Geers, C. Attanasio, M. B. S. Hesselberth, J. Aarts, and P. H. Kes, Phys. Rev. B **63**, 094511 (2001).

¹⁰M. H. Theunissen and P. H. Kes, Phys. Rev. B **55**, 15 183 (1997); for a comprehensive study, see M. H. Theunissen, Ph.D. thesis, University of Leiden, 1997.

¹¹F. Habbal and W. C. H. Joiner, J. Low Temp. Phys. **28**, 83 (1977);

J. D. Thompson and W. C. H. Joiner, Phys. Rev. B **20**, 91 (1979).

¹²P. H. Kes and C. C. Tsuei, Phys. Rev. B **28**, 5126 (1983).

¹³D. Babić, J. R. Cooper, J. W. Hodby, and Chen Changkang, Phys. Rev. B **60**, 698 (1999).

¹⁴M. Henny, S. Oberholzer, C. Strunk, and C. Schönberger, Phys. Rev. B **59**, 2871 (1999).

¹⁵A. I. Larkin and Yu. N. Ovchinnikov, in *Nonequilibrium Superconductivity*, edited by D. N. Lengenber and A. I. Larkin (North-Holland, Amsterdam, 1986).

¹⁶F. Lefloch, C. Hoffmann, and O. Demolliens, Physica C **319**, 258 (1999).

¹⁷C. M. Knoedler and R. F. Voss, Phys. Rev. B **26**, 449 (1982).

¹⁸E. Zeldov, D. Majer, M. Konczykowski, A. I. Larkin, V. M. Vinokur, V. B. Geshkenbein, N. Chikumoto, and H. Shtrikman, Europhys. Lett. **30**, 367 (1995).

¹⁹G. B. Lesovik, Pis'ma Zh. Éksp. Teor. Fiz. **49**, 513 (1989) [JETP Lett. **49**, 592 (1989)]; M. Büttiker, Phys. Rev. Lett. **65**, 2901 (1990).

²⁰For an overview of the various aspects of $1/f$ noise and resistance fluctuations, see, e.g., M. B. Weissman, Rev. Mod. Phys. **60**, 537 (1988).

²¹A. I. Bezuglyj and V. A. Shklovskij, Physica C **202**, 234 (1992).

²²From the LO theory it follows that out of equilibrium the vortex viscosity is velocity dependent and given by $\eta(v_\phi) = \eta_0 [1 + (v_\phi/v_\phi^*)^2]^{-1}$, where η_0 is the viscosity for small vortex velocities and v_ϕ^* a characteristic vortex velocity. Also, $A_c(v_\phi) = A_c(0) [1 + (v_\phi/v_\phi^*)^2]^{-1}$, which leads to $\eta(v_\phi) = \eta_0 A_c(v_\phi)/A_c(0)$. Therefore one should not confuse the vortex-size dependences of η_0 and $\eta(v_\phi)$: while η_0 is larger for smaller $A_c(0)$, $\eta(v_\phi)$ is smaller for smaller $A_c(v_\phi)$.

²³T. Matsuda, K. Harada, H. Kasai, O. Kanimura, and A. Tonomura, Science **271**, 1393 (1996).